



Wind Tunnel Study on Aerodynamic Particle Resuspension from Monolayer and Multilayer Deposits on Linoleum Flooring and Galvanized Sheet Metal

Brandon E. Boor,¹ Jeffrey A. Siegel,^{1,2} and Atila Novoselac¹

¹*Department of Civil, Architectural, and Environmental Engineering, Cockrell School of Engineering, The University of Texas at Austin, Austin, Texas, USA*

²*Department of Civil Engineering, The University of Toronto, Toronto, Ontario, Canada*

Resuspension is an important source of indoor particles and the amount of dust loading is an important factor in resuspension emission rates. Field studies have shown that light to heavy dust loads can be found in the indoor environment, on both the surfaces of flooring and ventilation ducts. These diverse particle deposits can be broadly classified as either a monolayer, in which particles are sparsely deposited on a surface, or a multilayer, in which particles are deposited on top of one another and there is particle-to-particle adhesion and interaction. This experimental wind tunnel study explores the role of the type of particle deposit on aerodynamic resuspension from linoleum flooring and galvanized sheet metal. Resuspension fractions are reported for both monolayer and multilayer deposits exposed to a wide range of air velocities. The type of particle deposit is found to strongly influence resuspension. In general, the results show that resuspension from multilayer deposits can occur at significantly lower velocities compared with monolayer deposits. For example, resuspension fractions at an air velocity of 5 m/s for the canopy layer of multilayer deposits were similar to those found for monolayer deposits at 50 m/s. Additionally, for multilayer deposits, resuspension fractions for the canopy layer increased with increasing dust load and negligible resuspension occurred along the surface layer. It was found that the relationship between the particle deposit height and the viscous sublayer thickness of the airflow can help explain the differences in resuspension that were observed between the two types of deposits. The impact of the type of particle deposit on

resuspension may have important implications for resuspension in the indoor environment, where a diversity of deposits can be found.

[Supplementary materials are available for this article. Go to the publisher's online edition of *Aerosol Science and Technology* to view the free supplementary files.]

INTRODUCTION

Resuspension is an important secondary source of particles in the indoor environment and has been found to be associated with convective airflow in ventilation ducts (Krauter and Biermann 2007; Wang et al. 2012) and human activities indoors (Thatcher and Layton 1995; Ferro et al. 2004; Qian and Ferro 2008; Tian et al. 2011; Shaughnessy and Vu 2012). Particle resuspension induced by aerodynamic removal forces can be influenced by numerous variables. Previous experimental wind tunnel studies have demonstrated the important role of a variety of parameters on resuspension, including particle size and air velocity (Corn and Stein 1965; Wu et al. 1992; Nicholson 1993; Braaten 1994; Ibrahim et al. 2003; Jiang et al. 2008; Mukai et al. 2009; Goldasteh et al. 2012b); surface material and roughness (Wu et al. 1992; Nicholson 1993; Gomes et al. 2007; Jiang et al. 2008; Mukai et al. 2009; Goldasteh et al. 2012b; Kassab et al. 2013); particle composition (Wu et al. 1992; Braaten 1994; Ibrahim et al. 2003; Goldasteh et al. 2012a); characteristics of the airflow such as acceleration (Wu et al. 1992; Nicholson 1993; Ibrahim et al. 2003), turbulence (Ibrahim et al. 2004; Mukai et al. 2009), exposure time (Ibrahim et al. 2003); and relative humidity and residence time (Ibrahim et al. 2004). Particle resuspension may also be strongly dependent on whether the deposit is a monolayer or a multilayer (Boor et al. 2013). A monolayer deposit is one in which particles are sparsely deposited on a surface, with negligible particle-to-particle contact. A multilayer deposit is a porous structure of particles deposited on top of one another, forming multiple layers. In these complex structures, the particle

Received 22 March 2013; accepted 30 March 2013.

Brandon E. Boor was supported by a National Science Foundation Graduate Research Fellowship under Grant No. DGE-1110007, a National Science Foundation IGERT Award under Grant No. DGE-0549428, and an American Society of Heating, Refrigerating, and Air-Conditioning Engineers Graduate Student Grant-In-Aid. The authors would like to thank the Microscopy and Imaging Facility of the Institute for Cellular and Molecular Biology at The University of Texas at Austin for providing access to the fluorescence stereomicroscope used in this research.

Address correspondence to Brandon E. Boor, Department of Civil, Architectural, and Environmental Engineering, The University of Texas at Austin, 1 University Station C1752, Austin, TX 78712-1076, USA. E-mail: bboor@utexas.edu; atila@mail.texas.edu

resuspension process is heavily affected by particle-to-particle adhesion and interaction between the larger particle aggregates and the airflow.

The type of particle deposit is of particular relevance to resuspension in the indoor environment, where we see a diversity of dust loads and deposit structures. Boor et al. (2013) summarized field studies that reported dust loads on indoor surfaces. On hard flooring, dust loads were typically in the range of less than 0.1–1 g/m², with lighter and heavier dust loads frequently reported in the literature (Table 1 in Boor et al. 2013). In ventilation ducts, dust loads were found to range over several orders of magnitude, from less than 0.1 to greater than 100 g/m². The authors presented a simple scaling analysis that demonstrated that this wide range of dust loading represents both monolayer and multilayer deposits. The authors also summarized key findings from the experimental resuspension literature that highlighted important differences in the resuspension process between monolayer and multilayer deposits.

Only a few modeling and experimental wind tunnel studies have explored multilayer resuspension, including those by Fromentin (1989), Matsusaka and Masuda (1996), Lazaridis and Drossinos (1998), Chiou and Tsai (2001), Friess and Yadigaroglu (2001), Friess and Yadigaroglu (2002), Gac et al. (2008), and Nitschke and Schmidt (2010), among others. Collectively, these studies have identified several unique characteristics associated with resuspension from multilayer deposits, including the following:

- Particles from the canopy layer of a multilayer deposit resuspend at lower velocities relative to particles in layers closer to the surface (Lazaridis and Drossinos 1998; Friess and Yadigaroglu 2001).
- There are reduced adhesion forces between spherical particles compared with that between a particle and a flat deposition surface (Lazaridis and Drossinos 1998).
- Resuspension often occurs in the form of larger particle aggregates, which, when airborne, can subsequently break apart due to forces imparted by turbulent bursts (Matsusaka and Masuda 1996; Kurkela et al. 2006; Gac et al. 2008; Gotoh et al. 2011).
- Enhanced resuspension may occur due to possible saltation effects (Bagnold 1941; Fairchild and Tillery 1982; Shao et al. 1993; Kok et al. 2012).
- The deposit structure and porosity is dependent on the deposition mechanism, e.g., gravitational settling may produce a “fluffy” deposit, compared with a “cake-like” deposit originating from inertial impaction (Friess and Yadigaroglu 2002).

Since both monolayer and multilayer deposits may be found on indoor surfaces, and there are fundamental differences in the resuspension process associated with both types of particle deposits, we expect the type of particle deposit to play an important role in the fraction of particles that resuspend from a surface. The primary aim of this investigation is to develop a

better understanding of the impact of the type of particle deposit on resuspension. An experimental methodology is developed to generate monolayer and multilayer deposits on linoleum flooring and galvanized sheet metal and to expose the deposits to a range of air velocities in a wind tunnel. The impact of the type of particle deposit is quantified by directly comparing resuspension fractions of fluorescent tracer particles from both deposits at different air velocities.

METHODOLOGY

An experimental methodology was developed to study aerodynamic resuspension from monolayer and multilayer particle deposits. For monolayer deposits, several variables were investigated: air velocity, particle size, relative humidity, and the type of indoor surface. Independent variables investigated for the multilayer deposits included dust loading, air velocity, type of indoor surface, and the layer location (canopy compared with surface, Figure 1). Two particle diameters were studied to explore the impact of particle size: 3 and 10 μm . Two flat indoor surfaces were examined for both deposits: linoleum, a common flooring material, and galvanized sheet metal, which is typically used to manufacture ventilation ducts. Two different seeding methods were developed to generate the monolayer and multilayer deposits. The deposits were then exposed to a range of air velocities in a wind tunnel. A fluorescence stereomicroscope was used to detect the deposited particles on the sample surface and a morphometry program was developed to count the number of particles. Figure 2 outlines the experimental sequence for both monolayer (Figure 2a) and multilayer deposits (Figure 2b).

The resuspension metric used in our investigation is an absolute resuspension fraction, Φ . Φ is defined as the change in seeding density before and after the seeded sample is exposed to a given flow condition in the wind tunnel, divided by the initial seeding density. It varies between 0, in which there is no

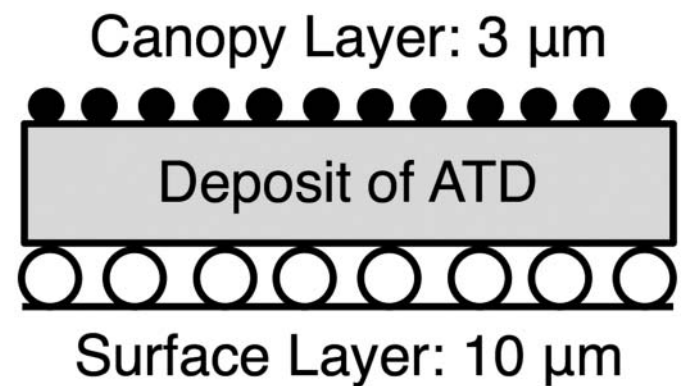


FIG. 1. Multilayer formation: canopy layer of 3- μm fluorescent particles, varying dust load deposit of Arizona Test Dust (ATD), and surface layer of 10- μm fluorescent particles.

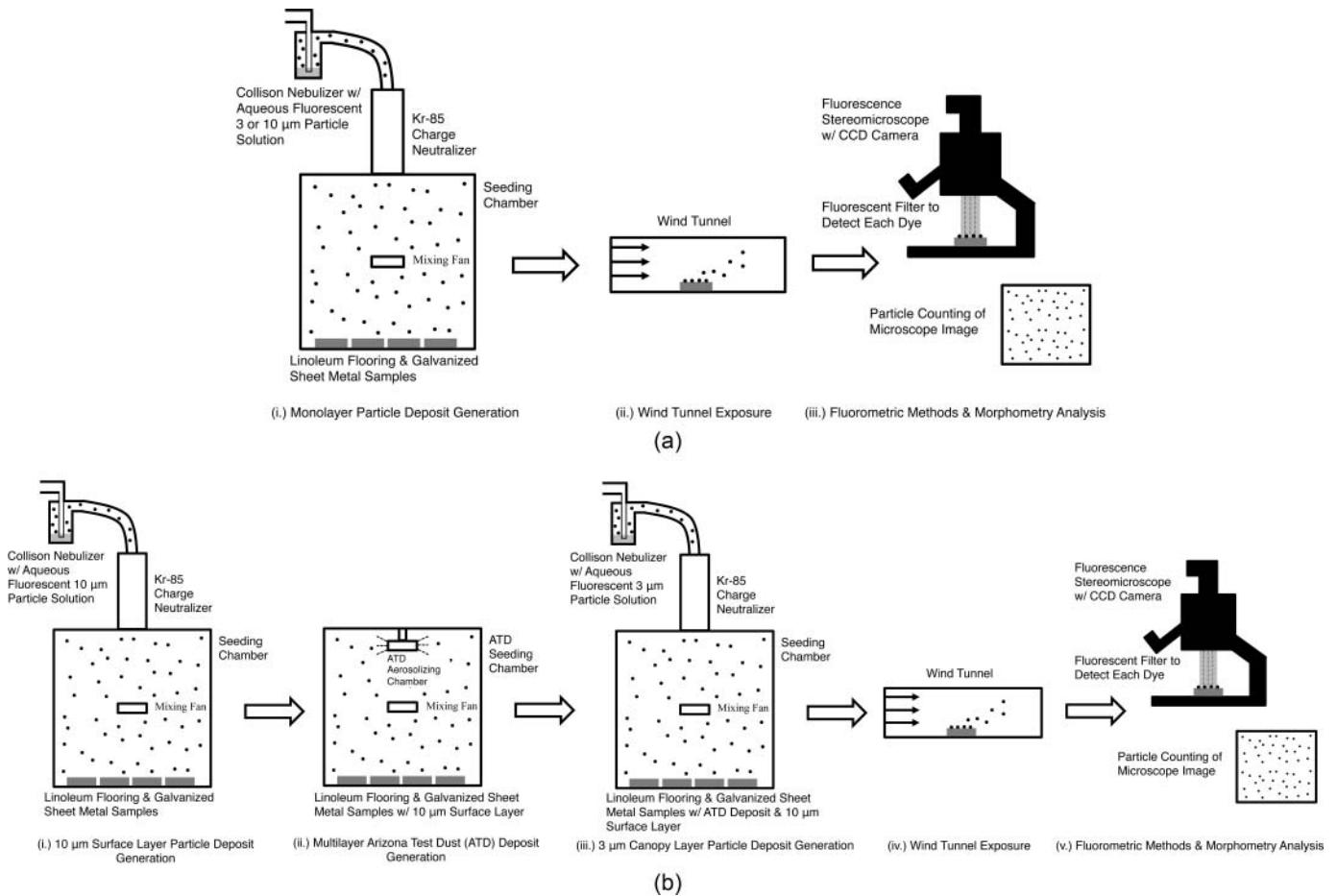


FIG. 2. Experimental sequence for (a) monolayer resuspension and (b) multilayer resuspension.

detectable resuspension, and 1, for maximum resuspension:

$$\Phi = \frac{\sigma_i - \sigma_f}{\sigma_i} \quad [1]$$

The initial, σ_i , and final, σ_f , seeding densities are expressed as the number of particles per unit area, particles/mm². The absolute resuspension fractions presented in our investigation are reported for a 100-s wind tunnel exposure time for both types of deposits.

Generation of Monolayer and Multilayer Particle Deposits

To generate the monolayer and multilayer deposits, two different seeding methods were employed. An aqueous solution of internally dyed, spherical polystyrene fluorescent particles (Thermo Scientific Inc., Waltham, MA, USA; density of 1060 kg/m³) was used to generate a sparse monolayer deposit. To easily distinguish between particle sizes and to forgo actual measurement of individual particles during microscopy analysis, a specific fluorescent dye was used to represent each particle size: red dye for 3 μm and green dye for 10 μm. The actual size of the supplied particles was verified via air sam-

pling with an aerodynamic particle sizer (TSI Inc., Shoreview, MN, USA; Model 3321). The fluorescent tracer particles were selected for their ease of generation; known, monodisperse size distribution; and detection via available instrumentation (e.g., Leica MZ16FA fluorescence stereomicroscope).

To generate the fluorescent particles for the monolayer deposit, the highly concentrated aqueous solution was first diluted with isopropyl alcohol (99% isopropyl alcohol, 1% deionized water). The diluted solution was then placed in a three-jet Collision Nebulizer (BGI Inc., Waltham, MA, USA; Model CN24). Filtered, pressurized air supplied by the laboratory's compressed air system was directed into the Collision Nebulizer at 127 kPa. Isopropyl alcohol droplets were subsequently generated, carrying the fluorescent particles with the effluent air stream. Because a residual electrostatic charge can accumulate on the particles within the glass jar of the nebulizer, the particle stream was passed through a Kr-85 Aerosol Charge Neutralizer (TSI Inc., Model 3012) to ensure all particles had a Boltzmann charge distribution.

The particle stream was then directed into a 50-L square box that served as a seeding chamber, with the samples positioned at the bottom (Figure 2a). A small mixing fan ensured the

chamber particle concentration remained well mixed, which was subsequently verified by assessing the seeding density uniformity among the samples (seeding density coefficient of variance among the samples was generally below 5%). Each sample was 4.5 × 4.5 cm in size and thoroughly cleaned before seeding with 99% isopropyl alcohol to minimize surface contamination and residual electrostatic charges. A steady-state particle concentration was reached in the seeding chamber after an injection period of 15 min (the nebulizer discharge produces an air exchange rate of approximately 6 h⁻¹), after which the particles were deposited via gravitational settling for approximately 6 h. Initial seeding densities for the 3- and 10- μm particles were (mean \pm SD) 67 \pm 19 and 0.73 \pm 0.16 particles/mm², respectively. Multiplying by the particle mass, the corresponding monolayer dust loads for the 3- and 10- μm particles were (mean \pm SD) 9.5 \pm 2.7 $\times 10^{-4}$ and 3.8 \pm 0.84 $\times 10^{-4}$ g/m², respectively. As shown in Boor et al. (2013), similar levels are reported for numerous monolayer wind tunnel studies.

The seeded samples were then placed in a 30-L conditioning chamber for 24 h prior to wind tunnel exposure, where the relative humidity was controlled and recorded with a HOBO data logger (HOBOWare Pro, Onset Computer Co., Bourne, MA, USA; Model U12-012). Two relative humidities were investigated: 35% and 70% (recorded values of 35% \pm 5% and 71% \pm 3%). The humidities were selected to represent both a dry and moist indoor environment.

To generate the multilayer deposit, two seeding chambers and three seeding stages were required (Figures 1 and 2b). First, a surface layer of 10- μm fluorescent particles was deposited in a sparse monolayer employing the aforementioned seeding method (initial seeding density of (mean \pm SD) 1.2 \pm 0.11 particles/mm²). The seeded samples were then placed in a second seeding chamber, where they were seeded with a multilayer deposit of polydisperse (1–20 μm) ISO 12103-1 A1 Ultrafine Arizona Test Dust (ATD; Powder Technology Inc., Burnsville, MN, USA). ATD was chosen over latex and silica microspheres and potassium chloride particles because it is both inexpensive and easily distributed along the sample surfaces in large quantities. An aerosolizing chamber was developed in which ATD was contained and an impinging jet of filtered air aerosolized the powder, which was then evenly dispersed through small inlets into the well-mixed seeding chamber. The ATD loading was measured gravimetrically with an analytical balance (Mettler-Toledo International Inc., Columbus, OH, USA; model AB135-5). Four ATD dust loads were examined (mean \pm SD): 6.23 \pm 1.10, 7.31 \pm 1.00, 13.21 \pm 3.33, and 20.25 \pm 1.91 g/m². The dust load of 6.23 g/m² was selected as the minimum dust load such that none of the 3- μm particles along the canopy layer would penetrate through the porous ATD to the surface. Trial experiments at dust loads below 5 g/m² were unsuccessful, as a pure canopy layer could not be achieved due to this penetration.

Ultrafine ATD has a mass median diameter of 4.5 μm and a bulk density of 500 kg/m³. Applying the simplified particle

deposit scaling analysis presented in Boor et al. (2013), and assuming a porosity of 0.75 corresponding to gravitational settling in the seeding chamber, all four ATD dust loads were verified as multilayer deposits. The deposit height was estimated to range from approximately 100 μm for a seeding density of 6.23 g/m² to 300 μm for a seeding density of 20.25 g/m² (Table S2 in the online supplemental information). The four dust loads are representative of levels found in the indoor environmental field studies summarized by Boor et al. (2013).

Lastly, the samples were seeded with a monolayer of 3- μm polystyrene fluorescent particles on the canopy of the existing multilayer deposit (initial seeding density of (mean \pm SD) 66 \pm 20 particles/mm²). The canopy layer was used to assess the impact of the multilayer deposit and particle-to-particle contact on the absolute resuspension fraction when compared with the monolayer experiments. The surface and canopy layers were distinguished by the different fluorescent dyes used for the 3- and 10- μm particles. It is important to note that the absolute resuspension fractions are only reported for these two layers and do not represent the total fraction of particles removed from the entire ATD deposit. All multilayer deposits were conditioned at a relative humidity of (mean \pm SD) 58% \pm 3% for 24 h prior to wind tunnel exposure (value based on laboratory ventilation conditions).

Wind Tunnel Exposure

Two wind tunnels were used to investigate resuspension from monolayer and multilayer particle deposits. Preliminary experiments for monolayer deposits found no detectable resuspension to occur for 3- and 10- μm particles at velocities below 25 m/s (Φ was \sim 0 between 5 and 20 m/s). To initiate aerodynamic resuspension of 3- and 10- μm particles, velocities greater than 25 m/s were required (also based on findings of Corn and Stein 1965 and Jiang et al. 2008 for particles near 10 μm in diameter; see Figure S1). To achieve air velocities of 25 m/s and greater, a high-velocity wind tunnel with a turbulent wall jet was designed and built. Computational fluid dynamics was used in the design of the high-velocity wind tunnel for the monolayer deposits. The wind tunnel was 20 cm in length, 5 cm wide, and 1.25 cm tall and was constructed with custom laser cut 0.635-cm-thick acrylic sheets. In order to generate high velocities above the sample surface, a wall jet was created via a 1 mm \times 5 cm rectangular nozzle. The wall jet was found to produce a very uniform discharge over the sample surface and exhibited the characteristic profile for turbulent plane wall jets (Rajaratnam 1976). Additional details on the wind tunnel design can be found in Boor et al. (2011). For the multilayer deposits, where resuspension occurred at much lower air velocities (<25 m/s), a small-scale wind tunnel was used (Omega Engineering Inc., Stamford, CT, USA; Model WT-4401-S-110V). Additional information about this wind tunnel and the associated flow characteristics, including velocity and turbulence profiles, can be found in Mukai et al. (2009).

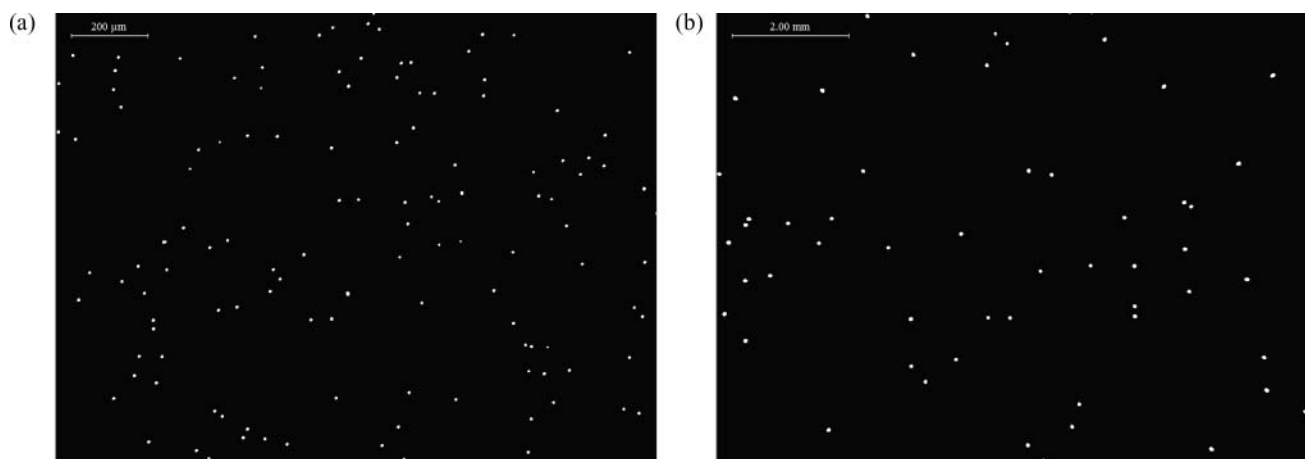


FIG. 3. Fluorescence stereomicroscope images: (a) 3- μm particles on galvanized sheet metal, image size: 1.55 \times 1.16 mm; (b) 10- μm particles on galvanized sheet metal, image size: 10.2 \times 7.66 mm.

Air velocity measurements were recorded with a one-dimensional constant-temperature hot-wire anemometer (MiniCTA probe 55P16, DanTec Dynamics, Skovlunde, DK). The anemometer took velocity measurements at a frequency of 1 kHz, which was necessary to capture the turbulent fluctuations of the high-velocity wall jet. For the monolayer deposits, three velocities, \bar{U} , were studied (mean \pm SD): 25 (actually 24.1 \pm 6.2), 50 (50.0 \pm 11.7), and 75 (73.9 \pm 17.7) m/s (velocity measurements taken at the approximate midpoint of the wall jet, \sim 1 mm above the surface). The acceleration of the flow was regulated by an automatically controlled needle valve and was approximately 2 m/s² for each of the three velocities. The turbulence intensities remained roughly the same for each velocity, and were approximately 26%, 23%, and 24% at 25, 50, and 75 m/s, respectively. For the multilayer particle deposits, the velocities studied were (nominally): 2.5, 5, 7.5, 10, 12.5, 15, 20, and 25 m/s; the acceleration was approximately 5 m/s²; and the average near-surface (\sim 1 mm) turbulence intensities were approximately 10%.

The exposure time for both the monolayer and multilayer deposits was 100 s. The exposure time can be divided into two temporal regimes: a period of flow acceleration, which was typically less than 30 s, depending on the final, steady-state velocity, and a period of steady-state flow. A few pilot experiments at low velocities found no significant change in particle resuspension between an exposure time of 10 s and 100 s, suggesting the majority of resuspension occurs during the acceleration period.

Fluorometric Methods and Morphometry Analysis

To determine the absolute resuspension fraction, Φ , for the monolayer particle deposits and the surface and canopy layers of the multilayer deposit, a fluorescence stereomicroscope (Leica MZ16FA, Leica Microsystems GmbH Wetzlar, HE, DE) equipped with a charge-coupled device (CCD) camera was used. The microscope and camera, along with morphometry analysis, were used to determine the seeding density, σ . The red 3- μm

and green 10- μm fluorescent particles were each detected using a different fluorescent filter and microscope and camera settings, as outlined in Table S1. The microscope was equipped with a MultiStep bi-directional scan feature through a motorized X/Y stage control that automatically scans a specified area and compiles the individual images into a larger, mosaic image. This allows a greater fraction of the sample area to be further analyzed with morphometry software. The camera settings were modified to obtain images with very high resolution and good contrast between the particle and background surface. As shown in Figure 3, a sparse monolayer deposit was verified by ensuring no particle-to-particle contact existed. (Note that the images in Figure 3 are only portions of the full, MultiStep images generated by the microscope for each sample.)

To count the number of particles within the area of the MultiStep image, and to determine the seeding density, a morphometric program was developed in the programming software MATLAB (MathWorks Inc., Natick, MA, USA). The grayscale image produced by the microscope camera software (Figure 3) was converted to a binary image of fully saturated white and black objects through a process known as thresholding. This helps isolate individual white objects, which represent individual particles. A threshold value of 5, on the standard grayscale of 0–255, was found to sufficiently isolate particles and remove any background noise produced by the inherent fluorescence of the linoleum flooring, galvanized sheet metal, or ATD in the case of the multilayer deposits. A histogram displaying the area distribution (in pixels²) was also generated to determine the impact of any outlying objects on the seeding density. Additionally, all microscope images were manually inspected to ensure that the white objects were isolated, circular in shape, and fully saturated. The accuracy and precision of the morphometry program was verified by comparing the seeding density with values derived from manual particle counting, as well as results from another morphometry program, MetaMorph (Molecular Devices, LLC, Sunnyvale, CA, USA). Lastly, no significant differences in

seeding densities were observed between the leading and trailing edges of the sample, suggesting minimal re-deposition of particles to the sample surface (although resuspended particles may have re-deposited further downstream of the sample within the wind tunnel, but this was not evaluated in this investigation).

Uncertainty and Quality Control

For the monolayer experiments, eight duplicate tests were performed for each indoor surface at each combination of air velocity and relative humidity (to determine σ_f). Twelve samples from each seeding batch were used to determine σ_i . For the multilayer experiments, six duplicate tests for each indoor surface and dust load were performed for a given air velocity (to determine σ_f). Six samples from each seeding batch were selected to determine σ_i for the 3- μm canopy layer and 10- μm surface layer, and six samples were selected to gravimetrically determine the dust load. Gross counts were used for both σ_i and σ_f , and particles were not tracked individually. To determine the uncertainty in Φ , the error in measuring both σ_i and σ_f was propagated. A bias error in the seeding density, based on the microscopy and morphometry analysis, of 5% (based on repeat analyses at different microscope and morphometric settings) was combined with the precision error of the sample population for a given set of conditions. In all results figures, the error bars represent the propagated uncertainty in Φ . Samples (approximately 10%) were excluded if the seeding density was 3 standard deviations from the mean, if there were noticeable deformations in the multilayer ATD dust load during the seeding process, or if the sample was improperly handled during wind tunnel exposure or microscopy analysis. Additionally, many trial experiments (data not reported here) were conducted for both the monolayer and multilayer (at approximately 20 g/m²) deposits when developing the experimental methodology to ensure adequate repeatability of the seeding methods and wind tunnel exposure.

RESULTS

Results for both the monolayer and multilayer deposits are shown in Figure 4. Each point on the plot represents the mean of one set of samples at the same conditions and the error bars represent the calculated error in Φ .

Monolayer Deposits

Resuspension of 3- and 10- μm particles from monolayer deposits is generally low across all three velocities studied, with Φ (mean \pm calculated error) ranging from 0.020 ± 0.018 to 0.048 ± 0.043 for 3- μm particles and from 0.039 ± 0.035 to 0.348 ± 0.131 for 10- μm particles (range across both surfaces and relative humidities), as shown in Figure 4a and b. As previously discussed, Φ was ~ 0 between 5 and 20 m/s. In general, Φ increases as velocity increases (beyond 25 m/s). At both 25 and 50 m/s, Φ generally does not exceed 0.10. At 75 m/s, Φ is found

to increase to levels beyond 0.10 for 10- μm particles, although no significant increase is observed for 3- μm particles. The size dependence of resuspension is also observed in Figure 4a and b. Φ is generally greater for 10- μm particles than for 3- μm particles at the same conditions. Φ is typically greater at 30% relative humidity compared with 75% relative humidity. On average, for 3- μm particles, Φ is 1.4 times greater at a relative humidity of 30% when compared with 75%. For 10- μm particles, a moderately stronger dependence on relative humidity is observed, with Φ increasing by a factor of 1.7 due to a reduction in relative humidity from 75% to 30%. The type of indoor surface also influenced resuspension from monolayer deposits. On average, for all velocities and at both relative humidities, Φ is 1.2 times greater for 3- μm particles on linoleum flooring when compared with galvanized sheet metal and 1.6 times greater for 10- μm particles.

Multilayer Deposits

Resuspension from multilayer deposits is found to be considerably different than resuspension from monolayer deposits. Numerous variables, including the dust loading, air velocity, the type of indoor surface, and the layer, are all found to influence resuspension to varying extents. The results in Figures 4c and d show that resuspension from the 3- μm canopy layer of multilayer deposits increases as the dust load increases. As with the monolayer deposits, resuspension from the 3- μm canopy layer generally increases with an increase in velocity. The impact of velocity is strongly coupled with the level of dust loading, with the two heaviest dust loads showing a significant increase in resuspension between 5 and 7.5 m/s, and the two lightest dust loads exhibiting a steady increase in resuspension with increasing velocity from 2.5 to 12.5 m/s. The impact of the surface appears to be small for resuspension from the canopy layer. Φ does not vary significantly between galvanized sheet metal and linoleum flooring for all four ATD dust loads. This makes sense given that the primary resuspension layer is the dust layer and not the surface material.

Resuspension is significantly greater for the 3- μm canopy layer of the multilayer deposit than for the 10- μm surface layer (surface layer results not reported in Figure 4). Φ for the surface layer is typically near 0 for all cases studied, with the exception of the lightest loading of 6.23 g/m². For many cases, the 10- μm particles along the surface layer are completely covered by ATD and could not be detected via fluorescence microscopy. Thus, Φ could not be accurately determined for many cases and is assumed to be 0 when covered by layers of ATD. For the 6.23 g/m² dust load, Φ is computed for velocities above 5 m/s. The surface layers Φ are 0.043 ± 0.002 , 0.029 ± 0.017 , 0.051 ± 0.008 , 0.033 ± 0.002 , 0.010 ± 0.014 , and 0.084 ± 0.048 for 7.5, 10, 12.5, 15, 20, and 25 m/s, respectively (average between both surfaces).

Resuspension occurs at significantly lower velocities for the multilayer deposits than for the monolayer deposits. For ATD

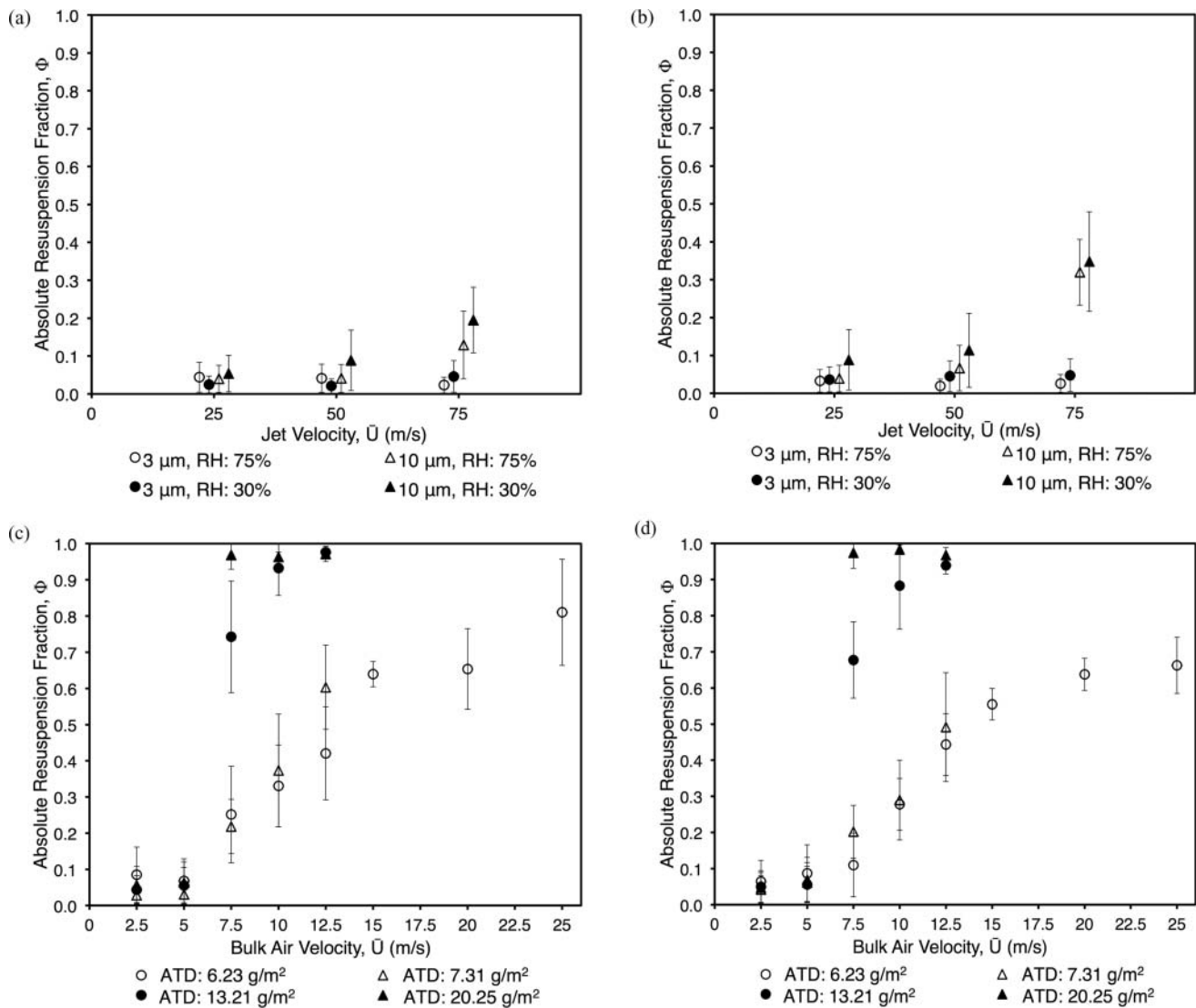


FIG. 4. Absolute resuspension fractions, Φ , for (a) monolayer deposit on galvanized sheet metal, (b) monolayer deposit on linoleum flooring, (c) 3- μm canopy layer of multilayer deposit on galvanized sheet metal, and (d) 3- μm canopy layer of multilayer deposit on linoleum flooring.

dust loads of 13.21 g/m^2 and 20.25 g/m^2 , Φ exceeds 0.883 ± 0.120 for the canopy layer of 3- μm particles at 10 m/s, whereas for the monolayer deposits, the highest achieved resuspension was for 10- μm particles at 75 m/s (Φ of 0.348 ± 0.131 for linoleum flooring at 30% relative humidity). Resuspension from multilayer deposits achieves similar levels at 5 m/s as those observed for monolayer deposits at 50 m/s. The average canopy layer Φ across all ATD dust loads at 5 m/s is 0.061 ± 0.015 and the average Φ for a monolayer of 3- μm particles is 0.032 ± 0.012 at 50 m/s, and for a monolayer of 10- μm particles, is 0.078 ± 0.027 . Thus, there is an apparent order of magnitude difference in the velocities required to resuspend similar levels of particles from the canopy layer of multilayer deposits and particles from monolayer deposits.

DISCUSSION

Resuspension was found to be considerably greater for multilayer deposits than for monolayer deposits. The findings of this investigation can be explained by considering the fundamental differences in the resuspension process between the two types of deposits. A detailed discussion of the unique attributes of resuspension from monolayer and multilayer deposits can be found in Boor et al. (2013), who summarize findings of the resuspension literature that address the key variables that impact resuspension from both types of deposits. The enhanced resuspension from multilayer deposits compared with monolayer deposits is likely due to reduced particle-to-particle adhesion forces, resuspension in the form of larger aggregates, and possible saltation effects (Bagnold 1941; Fairchild and Tillery 1982; Shao et al.

1993; Matsusaka and Masuda 1996; Lazaridis and Drossinos 1998; Friess and Yadigaroglu 2001; Kurkela et al. 2006; Gac et al. 2008; Gotoh et al. 2011; Kok et al. 2012). Boor et al. (2013) also contains a discussion on how the deposit structure and dust load may have important implications for particle resuspension and transport in the indoor environment.

Impact of Particle Deposit Height and Viscous Sublayer Thickness on Resuspension

Resuspension from both monolayer deposits and the canopy layer of multilayer deposits appears to be dependent on the relationship between the particle deposit height, δ (as defined in Boor et al. 2013), and the thickness of the viscous sublayer, y_{VSL} . δ for each of the four ATD dust loads was approximated using the scaling analysis presented in Boor et al. (2013), along with the known physical properties of ATD, and assuming that the deposit has a porosity of 0.75 due to gravitational settling in the seeding chamber. For the monolayer deposits, δ is simply equal to the diameter of deposited particles, either 3 or 10 μm . Additionally, y_{VSL} (μm) was approximated for each air velocity studied by applying the scaling relationship presented in Bejan (2004):

$$y_{VSL} \sim C \frac{\nu}{\bar{U}}, \quad [2]$$

where \bar{U} is the free-stream velocity (m/s), ν is the kinematic viscosity of air ($1.5 \times 10^{-5} \text{ m}^2/\text{s}$ at 20°C), and C is a unit-specific, dimensionless constant ($\sim 10^8$ for the units above). δ for each ATD dust load and monolayer deposit, and y_{VSL} for all velocities studied, are reported in Tables S2 and S3 in the online supplemental information. Although the values for both δ and y_{VSL} are based on simplified approximations, they still provide a good starting point for the following analysis.

Using Equation (2), the ratio of δ to y_{VSL} was determined for all monolayer and multilayer cases. Figure 5 shows the dependence of Φ , for both the monolayer deposits and canopy layer of the multilayer deposits, on the ratio of δ to y_{VSL} . An approximate logistic relationship was observed between Φ and δ/y_{VSL} . Similar logistic trends can be observed between Φ and the bulk air velocity in the monolayer wind tunnel studies of Ibrahim et al. (2003), Ibrahim and Dunn (2006), and Jiang et al. (2008), and between Φ and the volumetric airflow rate in the multilayer investigation of Gac et al. (2008). By fitting a logistic curve to all data points in Figure 5, the following empirical relationship between Φ and δ/y_{VSL} was determined:

$$\Phi \left(\frac{\delta}{y_{VSL}} \right) = \frac{K}{1 + e^{-r \left[\left(\frac{\delta}{y_{VSL}} \right) - \left(\frac{\delta}{y_{VSL}} \right)_0 \right]}}, \quad [3]$$

where K , r , and $(\delta/y_{VSL})_0$ are parameters determined through a least squares solution in MATLAB (MathWorks Inc.). K was found to be 0.99, r to be 3.51, and $(\delta/y_{VSL})_0$ to be 0.98. The correlation coefficient between the empirical relationship and

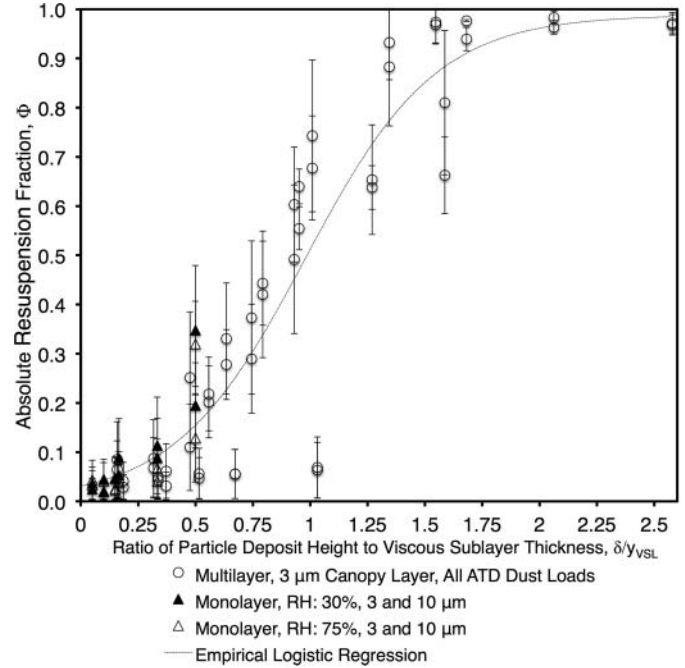


FIG. 5. Relationship between the absolute resuspension fraction, Φ , of both monolayer deposits and the canopy layer of multilayer deposits with the ratio of δ to y_{VSL} . Additionally, the empirical relationship derived for $\Phi(\delta/y_{VSL})$ is presented (Equation (3)).

measured data was found to be 0.938 (along with a root mean square error of 0.12), suggesting a strong, positive correlation between Φ and δ/y_{VSL} . The purpose of the empirical relationship, presented by Equation (3), is to help demonstrate that, for the data set presented in our investigation, there is an approximate logistic relationship between resuspension and the ratio of δ to y_{VSL} .

Observing the logistic trend presented in Figure 5, Φ grows exponentially to a δ/y_{VSL} of unity, after which its growth rate slows and it begins to asymptotically approach 1. For small values of δ/y_{VSL} , minimal resuspension was found to occur. When the particle deposit is completely immersed in the viscous sublayer ($y_{VSL} \gg \delta$), as is the case for monolayer deposits at low velocities, particles will not experience the enhanced removal associated with frequent collisions with turbulent eddies, and resuspension only occurs due to the periodic penetration of turbulent bursts from the fully turbulent sublayer (Cleaver and Yates 1973; Braaten et al. 1990; Jurcik and Wang 1991). As δ begins to approach y_{VSL} , a sharp increase in Φ is observed. As δ/y_{VSL} approaches unity (Figure 5), where we observe an inflection point in Φ 's dependence on δ/y_{VSL} , the edge of y_{VSL} is at roughly the same height as the particle deposit. $(\delta/y_{VSL})_0$ is the actual location of the inflection point, 0.98, where $\Phi \sim 0.5$. This was only achieved for the multilayer deposits, as the velocities studied for the monolayer deposits (25–75 m/s) were not large enough to reduce y_{VSL} to a height equivalent to that of the particles (3 and 10 μm).

Beyond a δ/y_{VSL} of unity, where the height of the deposit begins to surpass y_{VSL} and enter the fully turbulent sublayer, very high levels of resuspension are achieved and Φ begins to asymptotically approach 1. We can expect that at increasingly larger values of δ/y_{VSL} , due to an increase in bulk air velocity and/or an increase in the dust load, Φ will remain near 1 and the canopy layer will be completely resuspended. When increasing fractions of the multilayer particle deposit enter the fully turbulent sublayer, they likely experience the enhanced removal forces associated with turbulent eddies.

The concept of δ/y_{VSL} can help explain the role of the level of dust loading on resuspension from multilayer deposits. For velocities between 2.5 and 12.5 m/s, Φ was found to increase with dust loading from 6.23 to 20.25 g/m². As dust load increases, δ is expected to increase, and therefore, the ratio of δ/y_{VSL} for a given air velocity. Gomes et al. (2007) studied resuspension from dust loads of 0.5 and 2.5 g/m² and observed more particles to resuspend at the higher dust loading. A wind tunnel study by Nitschke and Schmidt (2010) found resuspension to generally increase with dust loading. Between an exposure time of 3 and 8 s, Φ increased as the dust load increased from 6.5 to 14 g/m² for both steel and PMMA surfaces. The findings of both Gomes et al. (2007) and Nitschke and Schmidt (2010) agree favorably with our investigation and help demonstrate the dependence of resuspension on the dust load, and therefore, δ .

The ratio of δ/y_{VSL} can also increase due to an increase in the air velocity (decreasing y_{VSL}). Our investigation found Φ to be strongly dependent on the air velocity and increase with increasing velocity. Fromentin (1989) found a similar trend for heavy multilayer deposits of 100–1000 g/m² and observed a significant increase in the resuspension flux by increasing the bulk air velocity from 8.5 to 20 m/s. Huang et al. (2005) and Matsusaka and Masuda (1996) observed similar trends in their respective wind tunnel studies.

Limitations of the Present Investigation

The focus of this study was to make direct comparisons of resuspension fractions between monolayer and multilayer deposits on indoor surfaces exposed to a range of air velocities in a wind tunnel, and not necessarily simulate realistic conditions under which resuspension occurs in the indoor environment. This investigation highlighted the important role of the type of particle deposit on aerodynamic resuspension from indoor surfaces, although it is important to discuss several limitations of this research. The wind tunnel resuspension experiments focused solely on aerodynamic-induced resuspension, whereby the airflow was accelerated at a nearly constant rate to some steady-state velocity. For flow in ventilation ducts, it would be expected that resuspension occurs primarily due to aerodynamic removal forces, although vibrational forces may be present. Particle deposits may be exposed to periods of high acceleration when a ventilation system cycles on and off, depending on the nature of the fan speed control. In addition, the turbulence of the airflow may vary considerably over different ventilation duct el-

ements, such as duct bends and irregularly shaped flex duct. For resuspension from flooring, airflow associated with the downward foot motion is likely very impulsive with high acceleration (Khalifa and Elhadidi 2007). Resuspension due to human activity may also generate additional removal forces, such as mechanical forces, due to surface vibrations, and electrostatic forces associated with the walking process (Gomes et al. 2007; Hu et al. 2008; Qian and Ferro 2008). The impact of airflow acceleration, turbulence levels, and additional removal mechanisms were not considered in this investigation, although these variables may have significant impact on resuspension under real conditions in the indoor environment.

The spherical fluorescent particles used in this investigation do not necessarily represent particles found in the indoor environment, which may vary considerably in their shapes, surface characteristics, and material compositions. However, they provide a basis to compare resuspension between two types of particle deposits. As such, the resuspension fractions provided in this investigation are used solely to compare monolayer and multilayer deposits, and do not necessarily represent resuspension fractions of actual indoor particles from indoor surfaces. It would be expected that resuspension may increase for irregularly shaped particles, such as spores, which have reduced contact area, and likely reduced adhesion, with deposition surfaces relative to spherical particles (Wu et al. 1992; Goldasteh et al. 2012a). Additionally, indoor particle deposits have a wide range of polydisperse size distributions (Boor et al. 2013), which may also influence resuspension.

SUMMARY

An experimental methodology was developed to determine aerodynamic resuspension from both monolayer and multilayer deposits on indoor surfaces. Resuspension was found to be strongly dependent on the type of particle deposit, with significantly greater levels of resuspension observed from multilayer deposits compared with monolayer deposits. Resuspension fractions at an air velocity of 5 m/s for the canopy layer of multilayer deposits were similar to those found for monolayer deposits at 50 m/s. Additionally, for monolayer deposits, resuspension fractions increased with increasing particle size and air velocity, and for multilayer deposits, resuspension fractions for the canopy layer increased with increasing dust load and air velocity. Relative humidity, the type of indoor surface, and layer location were also found to influence resuspension. Through scaling analysis, a relationship was found between the particle deposit height and viscous sublayer thickness that can help explain why elevated resuspension was observed from multilayer deposits compared with monolayer deposits. Other unique attributes of multilayer resuspension, including reduced particle-to-particle adhesion, resuspension in the form of larger aggregates, saltation effects, and deposition structure and porosity, can help explain the enhanced resuspension that was observed. Future work should consider the impact of other removal mechanisms and airflow

and environmental parameters on resuspension from multilayer deposits.

REFERENCES

- Bagnold, R. A. (1941). *The Physics of Blown Sand and Desert Dunes*. Methuen & Co. Ltd., New York.
- Bejan, A. (2004). *Convection Heat Transfer*. John Wiley & Sons, Inc., New Jersey.
- Boor, B. E., Siegel, J. A., and Novoselac, A. (2011). Development of an Experimental Methodology to Determine Monolayer and Multilayer Particle Resuspension from Indoor Surfaces, in *ASHRAE Transactions: Proceedings of the 2011 ASHRAE Winter Conference*, Las Vegas, NV, 117(1), pp. 434–441 (paper ID: LV-11-C053).
- Boor, B. E., Siegel, J. A., and Novoselac, A. (2013). Monolayer and Multilayer Particle Deposits on Hard Surfaces: Literature Review and Implications for Particle Resuspension in the Indoor Environment. *Aerosol Sci. Technol.*, 47:831–847.
- Braaten, D. A. (1994). Wind Tunnel Experiments of Large Particle Reentrainment: Deposition and Development of Large Particle Scaling Parameters. *Aerosol Sci. Technol.*, 21:157–169.
- Braaten, D. A., Paw, U. K. T., and Shaw, R. H. (1990). Particle Resuspension in a Turbulent Boundary Layer – Observed and Modeled. *J. Aerosol Sci.*, 21:613–628.
- Chiou, S. F., and Tsai, C. J. (2001). Measurement of Emission Factor of Road Dust in a Wind Tunnel. *Powder Technol.*, 118:10–15.
- Cleaver, J., and Yates, B. (1973). Mechanism of Detachment of Colloidal Particles from a Flat Substrate in a Turbulent Flow. *J. Colloid Interface Sci.*, 44:464–474.
- Corn, M., and Stein, F. (1965). Re-Entrainment of Particles from a Plane Surface. *Amer. Ind. Hyg. Assoc. J.*, 26:325–336.
- Fairchild, C. L., and Tillery, M. J. (1982). Wind Tunnel Measurements of the Resuspension of Ideal Particles. *Atmos. Environ.*, 16:229–238.
- Ferro, A. R., Kopperud, R. J., and Hildemann, L. M. (2004). Source Strengths for Indoor Human Activities that Resuspend Particulate Matter. *Environ. Sci. Technol.*, 38:1759–1764.
- Friess, H., and Yadigaroglu, G. (2001). A generic Model for the Resuspension of Multilayer Aerosol Deposits by Turbulent Flow. *Nucl. Sci. Engr.*, 138:161–176.
- Friess, H., and Yadigaroglu, G. (2002). Modelling of the Resuspension of Particle Clusters from Multilayer Aerosol Deposits with Variable Porosity. *J. Aerosol Sci.*, 33:883–906.
- Fromentin, A. (1989). *Particle Resuspension from a Multilayer Deposit by Turbulent Flow*. Doctoral dissertation, Swiss Federal Institute of Technology, Zurich.
- Gac, J., Sosnowski, T., and Gradon, L. (2008). Turbulent Flow Energy for Aerosolization of Powder Particles. *J. Aerosol Sci.*, 39:113–126.
- Goldasteh, I., Ahmadi, G., and Ferro, A. (2012a). A Model for Removal of Compact, Rough, Irregularly Shaped Particles from Surfaces in Turbulent Flows. *J. Adhesion.*, 88:766–786.
- Goldasteh, I., Ahmadi, G., and Ferro, A. (2012b). Wind Tunnel Study and Numerical Simulation of Dust Particle Resuspension from Indoor Surfaces in Turbulent Flows. *J. Adhes. Sci. Technol.*, in press, doi:10.1080/01694243.2012.747729.
- Gomes, C., Freihaut, J., and Bahnfleth, W. (2007). Resuspension of Allergen-Containing Particles Under Mechanical and Aerodynamic Disturbances from Human Walking. *Atmos. Environ.*, 41:5257–5270.
- Gotoh, K., Matsuda, S., Yoshida, M., Oshitani, J., and Ogura, I. (2011). Experimental Investigation of Particle Resuspension from a Powder Layer Induced by an Ascending Flat Object. *Kagaku Kogaku Ronbun.*, 37:317–322 (in Japanese).
- Hu, B., Freihaut, J. D., Bahnfleth, W. P., and Thran, B. (2008). Measurements and Factorial Analysis of Micron-Sized Particle Adhesion Force to Indoor Flooring Materials by Electrostatic Detachment Method. *Aerosol Sci. Technol.*, 42:513–520.
- Huang, C. H., Lee, C. I., and Tsai, C. J. (2005). Reduction of Particle Reentrainment Using Porous Fence in Front of Dust Samples. *ASCE J. Environ. Engr.*, 131:1644–1648.
- Ibrahim, A. H., and Dunn, P. F. (2006). Effects of Temporal Flow Acceleration on the Detachment of Microparticles from Surfaces. *J. Aerosol Sci.*, 37:1258–1266.
- Ibrahim, A. H., Dunn, P. F., and Brach, R. M. (2003). Microparticle Detachment from Surfaces Exposed to Turbulent Air Flow: Controlled Experiments and Modeling. *J. Aerosol Sci.*, 34:765–782.
- Ibrahim, A. H., Dunn, P. F., and Brach, R. M. (2004). Experiments and Validation of a Model for Microparticle Detachment from a Surface by Turbulent Air Flow. *J. Aerosol Sci.*, 35:805–821.
- Jiang, Y., Matsusaka, S., Masuda, H., and Qian, Y. (2008). Characterizing the Effect of Substrate Surface Roughness on Particle–Wall Interaction with the Airflow Method. *Powder Technol.*, 186:199–205.
- Jurcik, B., and Wang, H. C. (1991). The Modelling of Particle Resuspension in Turbulent Flow. *J. Aerosol Sci.*, 22:S149–S152.
- Kassab, A. S., Ugaz, V. M., King, M. D., and Hassan, Y. A. (2013). High Resolution Study of Micrometer Particle Detachment on Different Surfaces. *Aerosol Sci. Technol.*, 47:351–360.
- Khalifa, H. E., and Elhadidi, B. (2007). Particle Levitation due to a Uniformly Descending Flat Object. *Aerosol Sci. Technol.*, 41:33–42.
- Kok, J. F., Parteli, E. J. R., Michaels, T. I., and Karam, D. B. (2012). The Physics of Wind-Blown Sand and Dust. *Rep. Prog. Phys.*, 75:1–72.
- Krauter, P., and Biermann, A. (2007). Reaerosolization of Fluidized Spores in Ventilation Systems. *Appl. Environ. Microbiol.*, 73:2165–2172.
- Kurkela, J. A., Brown, D. P., Raula, J., and Kauppinen, E. I. (2006). New Apparatus for Studying Powder Deagglomeration. *Powder Technol.*, 14:164–171.
- Lazaridis, M., and Drossinos, Y. (1998). Multilayer Resuspension of Small Identical Particles by Turbulent Flow. *Aerosol Sci. Technol.*, 28:548–560.
- Matsusaka, S., and Masuda, H. (1996). Particle Reentrainment from a Fine Powder Layer in a Turbulent Air Flow. *Aerosol Sci. Technol.*, 24:69–84.
- Mukai, C., Siegel, J. A., and Novoselac, A. (2009). Impact of Airflow Characteristics on Particle Resuspension from Indoor Surfaces. *Aerosol Sci. Technol.*, 43:1–11.
- Nicholson, K. (1993). Wind Tunnel Experiments on the Resuspension of Particulate Material. *Atmos. Environ. Part A. Gen. Topics*, 27:181–188.
- Nitschke, D., and Schmidt, E. (2010). Experimental Study and Modelling of the Resuspension of Settled Particles. *Chem. Ingen. Technik.*, 82:2119–2127 (in German).
- Qian, J., and Ferro, A. (2008). Resuspension of Dust Particles in a Chamber and Associated Environmental Factors. *Aerosol Sci. Technol.*, 42:566–578.
- Rajaratnam, N. (1976). *Turbulent Jets*. Elsevier Scientific Publishing Co., Amsterdam.
- Shao, Y., Raupach, M. R., and Findlater, P. A. (1993). Effect of Saltation Bombardment on the Entrainment of Dust by Wind. *J. Geophys. Res.*, 98:12,719–12,726.
- Shaughnessy, R., and Vu, H. (2012). Particle Loadings and Resuspension Related to Floor Coverings in a Chamber and in Occupied School Environments. *Atmos. Environ.*, 55:515–524.
- Thatcher, T. L., and Layton, D. W. (1995). Deposition, Resuspension, and Penetration of Particles Within a Residence. *Atmos. Environ.*, 29:1487–1497.
- Tian, Y., Sul, K., Howard-Reed, C., Leber, D., and Ferro, A. R. (2011). A Comparative Study of Estimating Particle Resuspension Rate Using a Consistent Test Mechanism, in *Proceedings of the 12th International Conference on Indoor Air and Climate*, Austin, TX, paper ID:584.
- Wang, S., Zhao, B., Zhou, B., and Tan, Z. (2012). An Experimental Study on Short-Time Particle Resuspension from Inner Surfaces of Straight Ventilation Ducts. *Build. Environ.*, 53:119–127.
- Wu, Y.-L., Davidson, C. I., and Russell, A. G. (1992). Controlled Wind Tunnel Experiments for Particle Bounceoff and Resuspension. *Aerosol Sci. Technol.*, 17:245–262.